Pharmaceutical Sciences and Drug Design
ISSN: 3062-4428
2025, Volume 5, Page No: 135-151

Available online at: www.galaxypub.co/page/journals

Galaxy Publication

Optimization of Adapalene Microsponge Fabrication Parameters and Evaluation of Their In Vitro Biological Efficacy

Marcus Silva[1]*, Thiago Rocha[1], Daniel Nunes[1]

[1]Department of Biotechnology, Faculty of Science, University of São Paulo, São Paulo, Brazil.

***E-mail** ✉ marcus.silva.br@gmail.com

Received: 03 April 2025; **Revised:** 12 August 2025; **Accepted:** 15 August 2025

ABSTRACT

This study aimed to investigate microsponges (MS) as a drug delivery system using Adapalene (ADA) as the model compound.A Plackett-Burman design was employed to identify the critical factors influencing ADA-MS formulation. Microsponges were prepared via the quasi-emulsion solvent diffusion technique. The independent variables examined included organic phase volume, sonication duration, stirring speed, drug loading percentage, polymer type, emulsifier concentration, and the method of organic phase addition. Dependent outcomes assessed were entrapment efficiency (E.E.%), production yield (P.Y.%), particle size (P.S.), and morphology. Selected ADA-loaded microsponges (ADA-MS) were further evaluated in vitro for cytotoxicity, cell viability post-UVA exposure, and antimicrobial efficacy.Results revealed that drug loading, polymer type, and surfactant concentration were the primary determinants of E.E.% and P.Y.%, whereas drug loading, stirring speed, and organic phase volume significantly influenced particle size and morphology. ADA-MS exhibited pronounced cytotoxicity against A431 and M10 cell lines, particularly when Eudragit RS100 was used as the polymer. Additionally, ADA-MS improved HFB-4 cell viability following UVA irradiation by 14–43%, notably with Ethyl Cellulose as the polymer. Incorporation into microsponges also enhanced ADA's antimicrobial activity against Propionibacterium acnes. The Plackett-Burman design effectively identified formulation parameters impacting ADA-MS quality, while ADA's in vitro biological activities were significantly enhanced through microsponge encapsulation, highlighting microsponges as a promising carrier system for ADA.

Keywords: UVA irradiation, Plackett-burman, Anticancer, Antibacterial

How to Cite This Article: Silva M, Rocha T, Nunes D. Optimization of Adapalene Microsponge Fabrication Parameters and Evaluation of Their In Vitro Biological Efficacy. Pharm Sci Drug Des. 2025;5:135-51. https://doi.org/10.51847/WmpWYgBkny

Introduction

Microsponges have gained considerable attention as drug delivery vehicles due to their numerous advantages. These systems are polymeric, highly porous, and spherical in shape, with particle sizes ranging from 5 to 300 µm [1]. The internal pore network of a microsponge is extensive—approximately 3 meters per particle—because of the large number of interconnected pores (for example, a 25 µm particle may contain up to 25,000 pores) [1, 2]. This unique structure allows microsponges to encapsulate a wide variety of active agents, either on their surface or within the particle matrix, facilitating controlled, site-specific delivery with reduced dosing and minimized side effects. Microsponges can be fabricated using the liquid–liquid suspension method or the emulsion solvent diffusion technique, both of which are straightforward, cost-effective, and adaptable to different polymers [3]. The most frequently used polymers in microsponge preparation are Ethyl Cellulose (EC) and Eudragit RS100 (EUD). Both polymers are hydrophobic, while EUD also exhibits slight hydrophilicity due to quaternary ammonium groups in its structure, and both enable matrix formation with controlled release characteristics dependent on their swelling behavior and permeability [4]. Nevertheless, multiple formulation parameters can influence microsponge properties and drug delivery efficiency, making a systematic screening essential to minimize variability [1–3, 5, 6].

Screening numerous formulation parameters through trial-and-error approaches is laborious, costly, and time-consuming [7]. Utilizing statistical design of experiments (DOE) offers a powerful strategy for analyzing multiple factors simultaneously while determining their influence on dependent responses [8]. DOE reduces the number of experiments needed, accelerates the study, and provides statistically reliable results [9]. Among DOE approaches, the Plackett–Burman design is particularly efficient for screening a large number of factors. It allows evaluation of up to eleven variables at two levels through twelve experimental runs, simplifying optimization by identifying the key sources of variability requiring further investigation [10–13].

Adapalene (ADA; 6-[3-(1-adamantyl)-4-methoxyphenyl] naphthalene-2-carboxylic acid) was selected as the model drug to assess the microsponge formulation process and encapsulation effects. ADA is a third-generation retinoid with high hydrophobicity and enhanced stability against light and oxidation compared to other retinoids [14]. Its mechanism involves selective binding to retinoic acid receptors (RAR), particularly RAR-γ in the epidermis and RAR-β in fibroblasts, forming a RAR-ADA complex that interacts with retinoid X receptors (RXR) to modulate gene transcription, inhibit cell proliferation, regulate differentiation, and modulate inflammation [15–17]. These mechanisms underlie ADA's dermatological effects, making it effective in the topical treatment of mild to moderate acne, supporting hair follicle differentiation, and contributing to depigmentation and anti-photoaging effects [18–20]. Emerging studies also highlight ADA's anticancer potential against various cell types, including colorectal, hepatoma, ovarian ES-2, cervical intraepithelial, HaCat, and melanoma cells [18, 21].

Although topical administration minimizes systemic toxicity [22], ADA can cause notable local side effects, such as photosensitivity, erythema, dryness, pruritus, stinging, and burning [18]. Thus, developing an advanced carrier system is critical to improve tolerability and reduce side effects, positioning ADA as an ideal candidate for investigating microsponge-based drug delivery.

This study focused on statistically evaluating the key parameters influencing ADA-loaded microsponge (ADA-MS) fabrication using the Plackett-Burman design. Additionally, the study aimed to explore how microsponges affect the in vitro biological activities of ADA, including cytotoxicity, UVA-induced effects on cell viability, and antimicrobial activity.

Materials and Methods

Materials

Adapalene (ADA) was provided by Borg Pharmaceutical Industries (Alexandria, Egypt), while Eudragit RS100 (EUD) was supplied by Evonik Operations GmbH (Essen, Germany). Ethyl Cellulose (EC) and Polyvinyl Alcohol (PVA) were sourced from Egyptian International Pharmaceutical Industries Co. (EIPICO, 10th of Ramadan City, Egypt). Dichloromethane was obtained from El-Nasr Pharmaceutical Chemicals Co. (Cairo, Egypt), and tetrahydrofuran from Fisher Scientific (Massachusetts, USA). All solutions were prepared using distilled water produced on-site (Aquatron Water Still, A4000D, UK).

Experimental design

To identify the critical factors affecting microsponge formulation, a Plackett-Burman design (PBD) was employed via Design-Expert® software (v.13.0.0, Stat-Ease, Inc., Minneapolis, MN, USA). Seven formulation parameters were investigated at two levels, as outlined in **Table 1**. Twelve experimental runs were conducted for ADA-loaded microsponge (ADA-MS) preparations, summarized in **Table 2**. The independent factors examined included: organic phase volume (A), sonication duration (B), stirring rate (C), drug loading percentage (D), polymer type (E), emulsifier concentration (F), and method of organic phase addition (G). Their effects were analyzed on key outcomes: entrapment efficiency (Y1), production yield (Y2), particle size (Y3), and microsponge morphology (Y4).

Table 1. Investigated variables in plackett-burman experimental design

Investigated Variables	Levels	
	−1	**1**
Volume of organic phase (mL) (A)	5	20
Sonication time (minutes) (B)	5	15
Stirring speed (rpm) (C)	500	1500
Drug percent (%) (D)	50	80

Polymer type (E)	Eudragit RS100	Ethyl Cellulose
Emulsifier concentration (%) (F)	0.1	0.5
Method of organic phase addition (G)	Portionwise	Dropwise
Dependant Variables	**Constrains**	
Entrapment efficiency (%) (Y1)	Maximize	
Production yield (%) (Y2)	Maximize	
Particle size (µm) (Y3)	Minimize	
Morphology (Y4)	Maximize	

Table 2. Composition of adapalene loaded microsponges and the observed values of the dependent responses

Formulae	A (mL)	B (min)	C (rpm)	D (%)	E	F (%)	G	Y1 (%) ± S.D.	Y2 (%) ± S.D.	Y3 (µm) ± S.D.	Y4
F1	5	15	1500	50	EC	0.5	DW	50.9 ± 3.7	54.4 ± 2	47.2 ± 16.7	2
F2	20	15	1500	50	EUD	0.1	DW	86.3 ± 2.3	62.3 ± 0.4	14.97 ± 4	3
F3	20	5	500	50	EC	0.1	DW	85 ± 3.3	85 ± 1.2	43.3 ± 4.65	1
F4	20	5	1500	80	EC	0.1	PW	96.6 ± 1.2	88 ± 0.8	30.27 ± 10.2	2
F5	5	15	1500	80	EUD	0.1	PW	92 ± 1.7	82.3 ± 1.3	31.32 ± 11.3	1
F6	5	5	500	50	EUD	0.1	PW	80.9 ± 2.1	68.8 ± 0.3	64.76 ± 8.25	3
F7	20	5	1500	80	EUD	0.5	DW	90.9 ± 1.9	86 ± 1	29.3 ± 6.7	3
F8	5	15	500	80	EC	0.1	DW	95.4 ± 1.1	81.3 ± 0.8	106.1 ± 23.1	1
F9	5	5	1500	50	EC	0.5	PW	50.9 ± 2.2	43.3 ± 2.2	29.4 ± 7.7	2
F10	5	5	500	80	EUD	0.5	DW	90.8 ± 1.5	87.3 ± 0.7	162.6 ± 37.4	1
F11	20	15	500	80	EC	0.5	PW	99.8 ± 0.5	93.1 ± 0.6	35.5 ± 11.2	1
F12	20	15	500	50	EUD	0.5	PW	38.5 ± 3.5	33.2 ± 1.3	26.3 ± 4.5	3

Notes: A: volume of organic phase; B: sonication duration; C: stirring speed; D: drug loading percentage; E: polymer type; F: emulsifier concentration; G: method of organic phase addition. Y1: entrapment efficiency; Y2: production yield; Y3: particle size; Y4: morphology.
Abbreviations: EC, Ethyl Cellulose; EUD, Eudragit RS100; DW, dropwise; PW, portionwise.

Preparation of adapalene-loaded microsponges

The twelve ADA-loaded microsponge formulations listed in **Table 2** were synthesized via the quasi-emulsion solvent diffusion technique [23]. ADA and the selected polymer were combined in ratios of 1:1 and 4:1, respectively, and dissolved in dichloromethane to generate the organic internal phase. This phase was sonicated for uniform dispersion using a bath sonicator (Elmasonic S60H, Germany). The aqueous external phase was prepared by dissolving the appropriate amount of PVA in 100 mL of distilled water, heating the solution to 70°C on a hotplate-magnetic stirrer (DAIHAN Scientific, Korea), and allowing it to cool to ambient temperature. The organic phase was then gradually incorporated into the aqueous phase under continuous stirring with an overhead stirrer (HS-30D, DAIHAN Scientific, Korea) at room temperature for 2 hours. The formed microsponges were separated by filtration through 0.45 µm Whatman filter paper, washed with distilled water, and dried in an oven at 50°C until no moisture remained. The dried microsponge powders were stored in sealed containers at room temperature for subsequent analyses.

Assessment of microsponge performance

The prepared microsponge formulations were evaluated for their entrapment efficiency (Y1), production yield (Y2), particle size (Y3), and morphological features (Y4).

Determination of Entrapment Efficiency (EE%) (Y1)

To quantify the amount of ADA encapsulated within the microsponges, a measured quantity of ADA-MS was dissolved in 10 mL tetrahydrofuran to break down the polymer matrix. The solution underwent sonication for 10 minutes, followed by filtration and appropriate dilution. ADA concentration was determined spectrophotometrically at 237 nm using a UV spectrophotometer (V-630, Jasco, Japan), with values calculated from a previously constructed calibration curve. Each measurement was repeated three times, and the entrapment efficiency percentage was computed using the standard formula [24].

$$EE(\%) = \frac{\mathrm{M}_{\mathrm{act}}}{\mathrm{M}_{\mathrm{the}}} \times 100 \quad (1)$$

In the equation for entrapment efficiency, Mact represents the actual amount of ADA present in the microsponge formulation, while Mthe denotes the theoretical drug content.

Production yield (P.Y.%) (Y2)

The production yield percentage was calculated by comparing the total weight of microsponges obtained to the combined weight of all starting materials. This value was determined using the following formula [25]:

Production Yield(%)=(practical mass of microspones)/(Theoretical mass (polymer+adapalene))×100 (2)

Particle size (Y3) and morphology (Y4)

The average particle size and surface characteristics of the prepared microsponges were evaluated using a Scanning Electron Microscope (SEM) (Thermo Scientific FEG SEM Quattro, USA). Samples were directly placed on SEM stubs without any conductive coating. Images were captured under a low vacuum at 10 kV accelerating voltage, and morphological consistency was verified by analyzing replicate samples [26]. Multiple magnifications were used to assess the microsponge structure. A scoring system was applied to describe morphology: 1 indicated a low number of regular spherical microsponges, 2 represented an intermediate number, and 3 corresponded to a high density of uniform spherical microsponges within the field.

Statistical analysis

The influence of formulation parameters on microsponge characteristics was visualized using standardized Pareto charts and response surface plots, allowing identification of statistically significant factors in the Plackett-Burman design. Analysis of variance (ANOVA) was conducted to determine the statistical relevance of the model, with a significance threshold set at $p < 0.05$. Regression analyses and graphical representations were generated using Design-Expert® software (v.13.0.0, Stat-Ease, Inc., Minneapolis, MN, USA).

In vitro biological activity of selected ADA-MS formulations

Biological evaluations were performed on selected ADA-loaded microsponge formulations: one prepared with Ethyl Cellulose (ADA-MS-EC) and another with Eudragit RS100 (ADA-MS-EUD), in comparison to free ADA. The assays included cytotoxicity against epidermoid carcinoma (A431) and melanoma (M10) cell lines, UVA photoprotection on normal melanocytes (HFB-4), and antimicrobial activity against Propionibacterium acnes.

Cytotoxicity assay

A431 and M10 cells were obtained from the American Type Culture Collection (ATCC, Rockville, MD) and cultured in DMEM supplemented with 10% fetal bovine serum, 10 µg/mL insulin, and 1% penicillin-streptomycin. Cells were maintained at 37°C in a humidified incubator with 5% CO_2. For testing, cells were seeded in 96-well plates for 24 hours to allow adhesion, then treated with serial concentrations of free ADA, ADA-MS-EC, or ADA-MS-EUD for 48 hours. Cell viability was determined using the MTT assay: 3-(4,5-dimethylthiazol-2-yl)-2,5-diphenyltetrazolium bromide was added and incubated for 4 hours, after which formazan crystals were solubilized with DMSO. Absorbance was measured at 570 nm (SunRise, TECAN, USA), and survival curves were generated to calculate IC50 values via non-linear regression using GraphPad Prism 8 software [21, 27].

UVA irradiation and cell viability

HFB-4 cells were seeded in 96-well plates for 24 hours, then treated with ADA or ADA-loaded microsponges (3–12 µg/mL) for 24 hours [28]. To evaluate photoprotection, cells were exposed to 64.8 J/cm² UVA radiation at 365 nm for 6 hours (UV lamp, Biotech, Spain) [29]. Post-irradiation, cell viability was assessed using MTT, with absorbance at 570 nm recorded. Relative viability was calculated compared to untreated controls. Data from at least three independent experiments were analyzed by one-way and two-way ANOVA, with $p < 0.05$ considered significant [30].

Antimicrobial activity

The antimicrobial effect of free ADA and ADA-MS formulations (ADA-MS-EC, ADA-MS-EUD) against P. acnes (ATCC 6919) was evaluated across concentrations of 6–500 µg/mL. Bacteria were cultured on reinforced clostridial medium (RCM) agar at 37°C for 48–72 hours. In 96-well plates, 100 µL RCM broth was added to each well, followed by 100 µL of ADA formulations, serially diluted two-fold in RCM. Cultures were inoculated with P. acnes suspension at 1×10^8 CFU/mL (half McFarland standard) and incubated anaerobically at 37°C. After 48 hours, bacterial growth was quantified via absorbance at 570 nm (BioTek ELX800, USA), and MIC values were determined. Linear regression analysis with 95% confidence intervals was performed using GraphPad Prism 8 software [31, 32].

Results and Discussion

Data modeling

Experimental design approaches such as the Plackett-Burman design (PBD) are highly effective for identifying key factors among numerous variables with minimal experimental runs [33]. In this study, PBD was applied to the most influential formulation parameters in microsponge preparation to maximize entrapment efficiency and production yield, minimize particle size, and optimize particle morphology. Twelve distinct experimental runs were generated.

As summarized in **Table 2 and Figure 1**, microsponge entrapment efficiency ranged from 38.48% to 99.76%, while production yield varied between 33.2% and 93.14%. Particle sizes spanned 14.97–162.6 µm, and morphology scores ranged from low (1) to high (3) homogeneity of spherical particles.

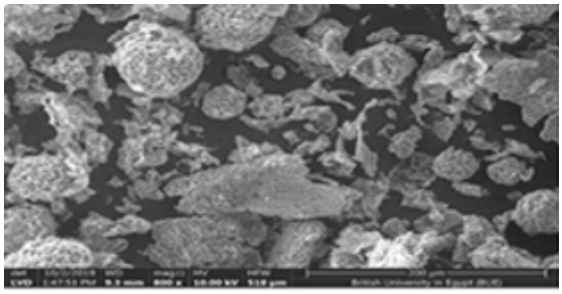

1a)

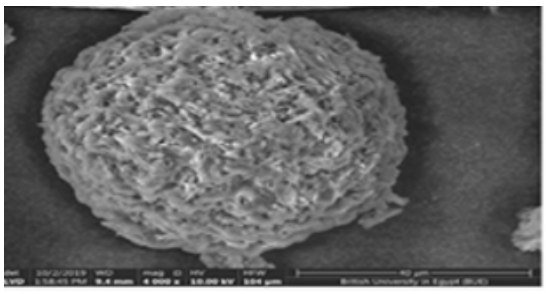

1b)

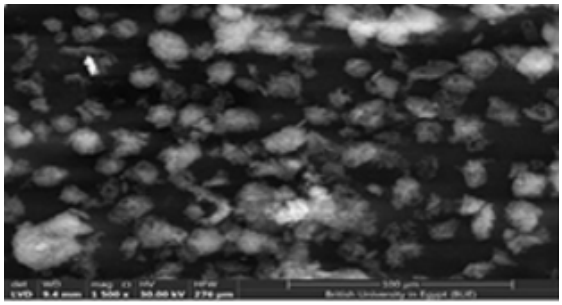

2a)

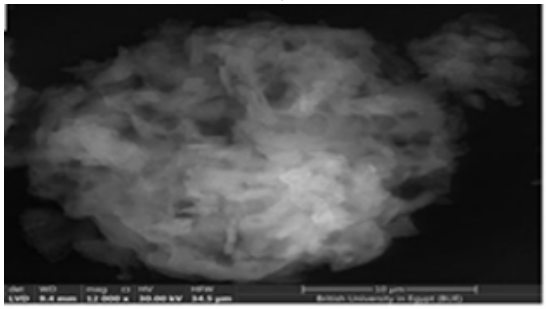

2b)

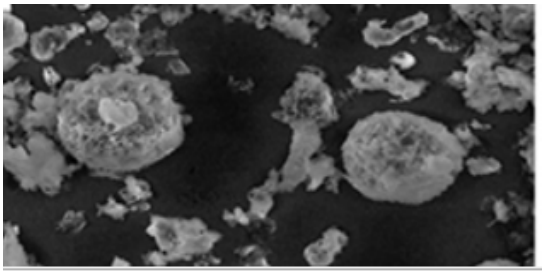

3a)

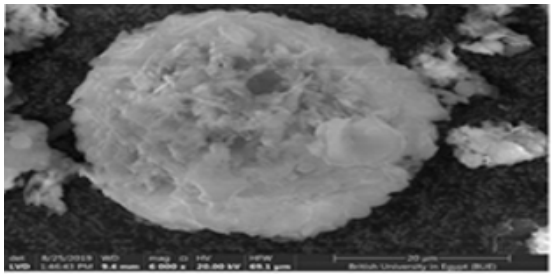

3b)

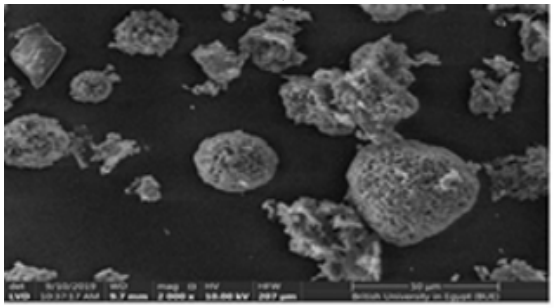

4a)

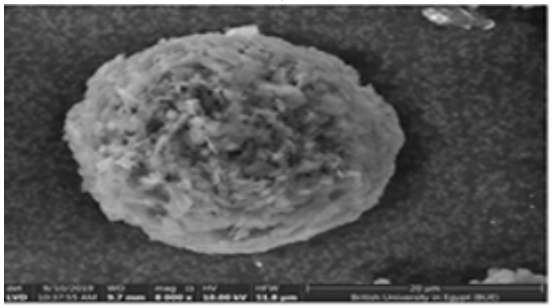

4b)

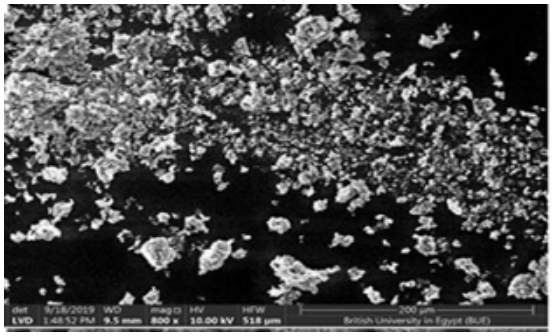

5a)

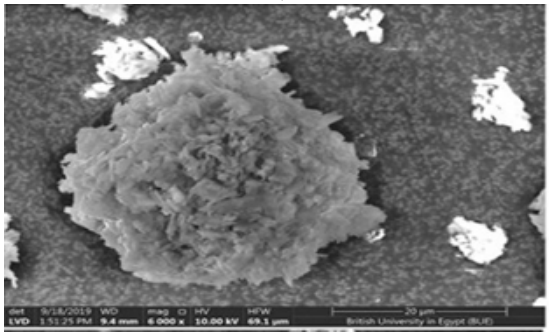

5b)

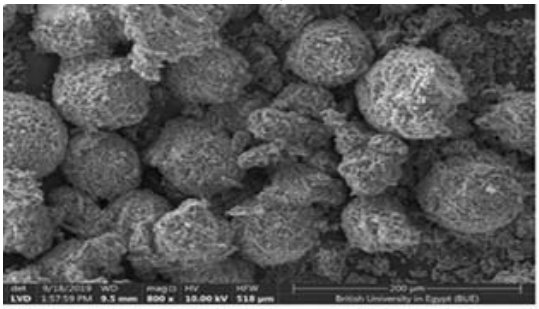

6a)

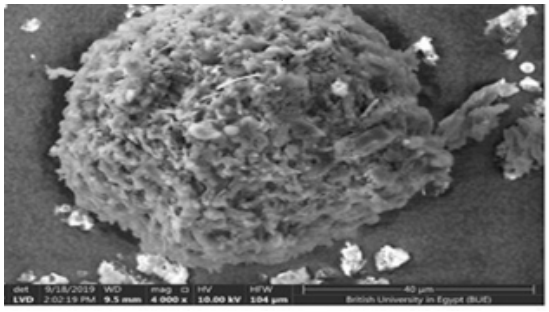

6b)

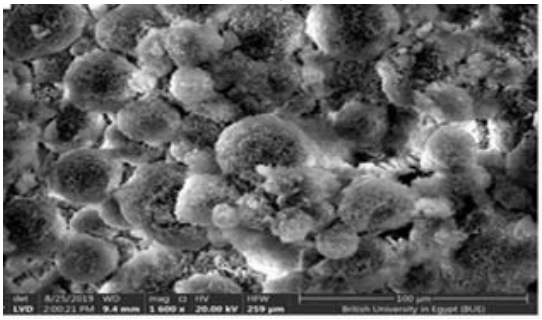

7a)

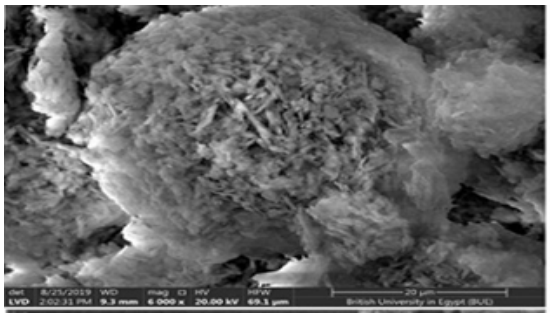

7b)

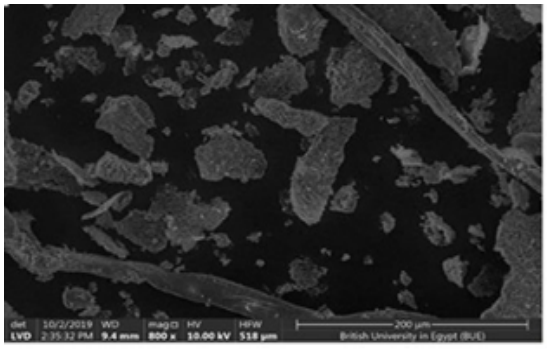

8a)

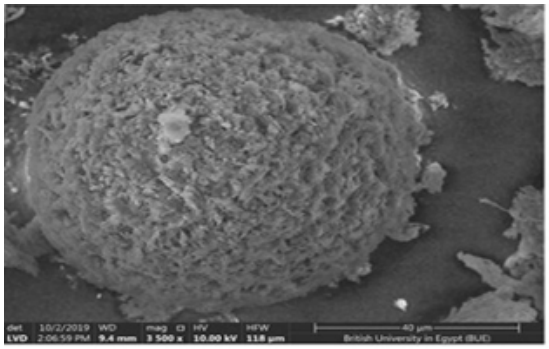

8b)

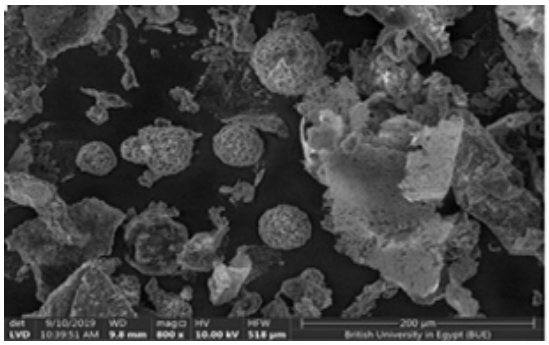

9a)

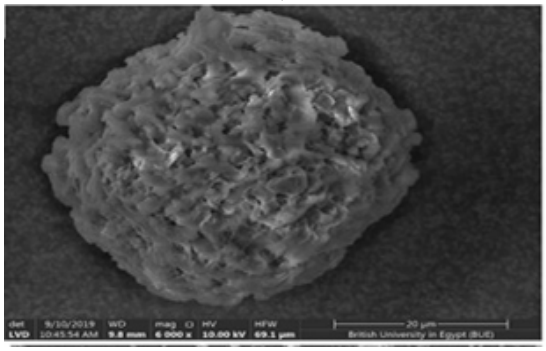

9b)

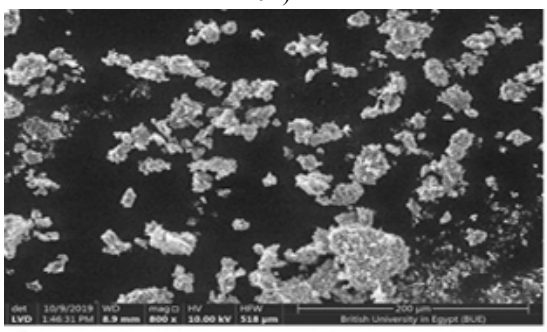

10a)

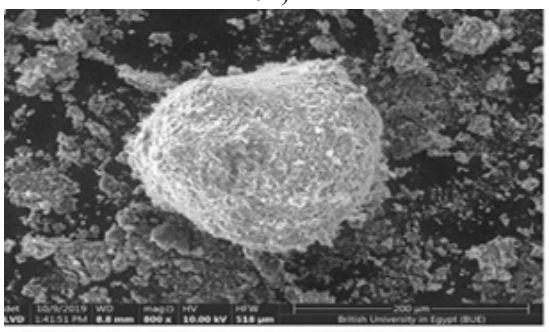

10b)

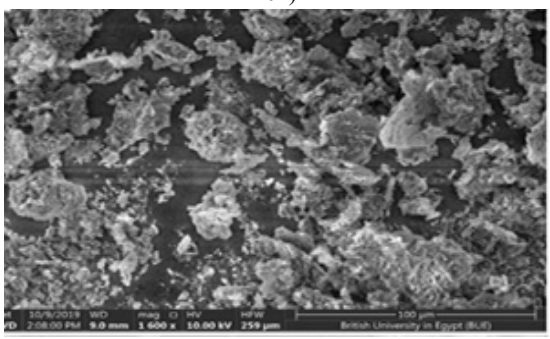

11a)

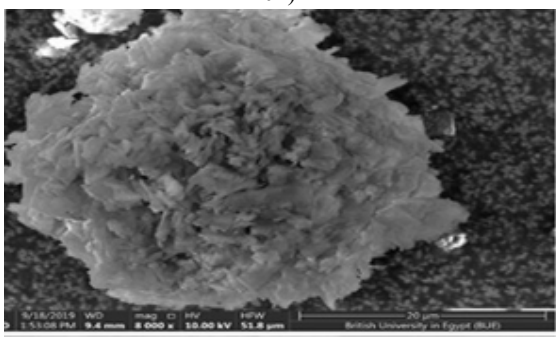

11b)

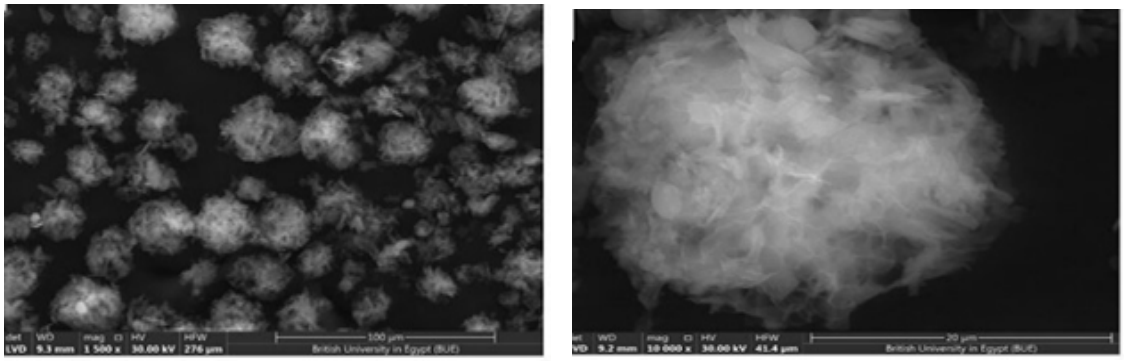

12a) 12b)

Figure 1. SEM micrographs of formulations f1 through f12. Panels 1a to 12a illustrate the overall field of microsponges, whereas panels 1b to 12b focus on individual microsponge particles.

Statistical evaluation of the responses using analysis of variance (ANOVA) is summarized in **Table 3**. Based on these results, all four response models were deemed suitable for exploring the design space. The experimental data were further used to generate polynomial equations, which are presented below in terms of coded variables:

$$Entrapment\ Efficiency\ \%\ (Y_1) = 79.81 - 1.05A + 1.39B + 2.18C + 14.41D + 4.00E - 9.54F - 0.96G + 12.23DF \quad (3)$$

$$Production\ Yide\ \%(Y_2) = 72.08 - 0.82A + 0.57B + 0.64C + 11.35D + 8.4E - 7.28F + 0.56G - 4.27BG + 10.22DF + 4.44FG \quad (4)$$

$$Particle\ size(Y_3) = 51.75 - 21.81A + 0.47B - 27.22C + 17.19D - 6.21E + 6.08F + 6.83G + 8.36AC - 17.62AF \quad (5)$$

$$Morphology(Y_3) = 1.92 + 0.25A + 0B + 0.37C - -0.75D - \ -0.083E + 2.9F - \ -0.17G + 0.62AC + 0.37AF \quad (6)$$

Table 3. Statistical analysis of variance (ANOVA) of the responses (Y1−Y4)

Independent Variable	Y1		Y2		Y3		Y4	
	Coefficient Estimate	**P-value**	**Coefficient Estimate**	**P-value**	**Coefficient Estimate**	**P-value**	**Coefficient Estimate**	**P-value**
Model		0.0004*		0.0314*		0.0293*		0.0814
A	−1.05	0.1211	−0.82	0.2356	−21.87	0.0112*	0.25	0.0955
B	1.39	0.0659	0.57	0.3039	−2.3	0.8831	0	1
C	2.18	0.0211*	0.64	0.2938	−27.22	0.009*	0.37	0.0565
D	14.41	<0.0001*	11.35	0.0165*	19.97	0.0263*	−0.75	0.018*
E	4	0.0039*	8.41	0.024*	−9	0.1607	−0.083	0.5
F	−9.54	0.0002*	−7.28	0.0234*	3.3	0.1439	0.29	0.0887
G	−0.69	0.2534	0.56	0.2826	9.62	0.1383	−0.17	0.2441
	(**DF**) 12.23	0.0003*	(**DF**) 10.22	0.0224*	(**AF**) −7.62	0.0369*	(**AC**) 0.62	0.0377*
R^2	0.9985		0.9998		0.9934		0.9813	
Adi. R^2	0.9947		0.9982		0.9638		0.8972	
Adeq. Percision	46.524		75.302		19.557		8.222	

SEE	1.52	0.83	12.94	0.29
MAE	78.81	72.08	51.75	1.92

Notes: *Indicates significance at $p < 0.05$. A: organic phase volume; B: sonication duration; C: stirring speed; D: drug loading percentage; E: polymer type; F: emulsifier concentration; G: method of organic phase addition. Y1: entrapment efficiency; Y2: production yield; Y3: particle size; Y4: morphology.

Effect of formulation parameters on entrapment efficiency (Y1)

The entrapment efficiency (EE%) of the ADA-loaded microsponge formulations showed a wide range, from 38.48% in F12 to 99.76% in f11 **(Table 2).** As indicated in **Table 3**, increasing the drug loading percentage had a significant positive influence on EE%. This effect can be attributed to the fact that higher drug content reduces the proportion of polymer, lowering the viscosity of the medium and allowing easier diffusion of ADA, which facilitates the formation of a more flexible polymeric coating [34]. Among the polymers tested, Ethyl Cellulose was more favorable, likely due to differences in polymer structure, swelling behavior, and corresponding drug-loading capacity [35–37].

Conversely, higher concentrations of the emulsifier (PVA) exhibited a significant negative effect on EE%. This may result from increased PVA levels enlarging microsponge pore size, which promotes drug leaching [38, 39]. Additionally, ADA's hydrophobic nature combined with the non-ionic character of PVA means that at high PVA concentrations, hydrophobic domains may form, solubilizing portions of ADA and reducing the entrapped drug content [40]. Using lower PVA amounts decreases drug solubility in the external phase, thereby minimizing drug loss [24, 40].

Furthermore, the interaction between drug percentage and emulsifier concentration (D × F), illustrated in **Figure 2a**, demonstrated a significant positive effect on entrapment efficiency, highlighting the importance of balancing these two factors for optimal drug loading.

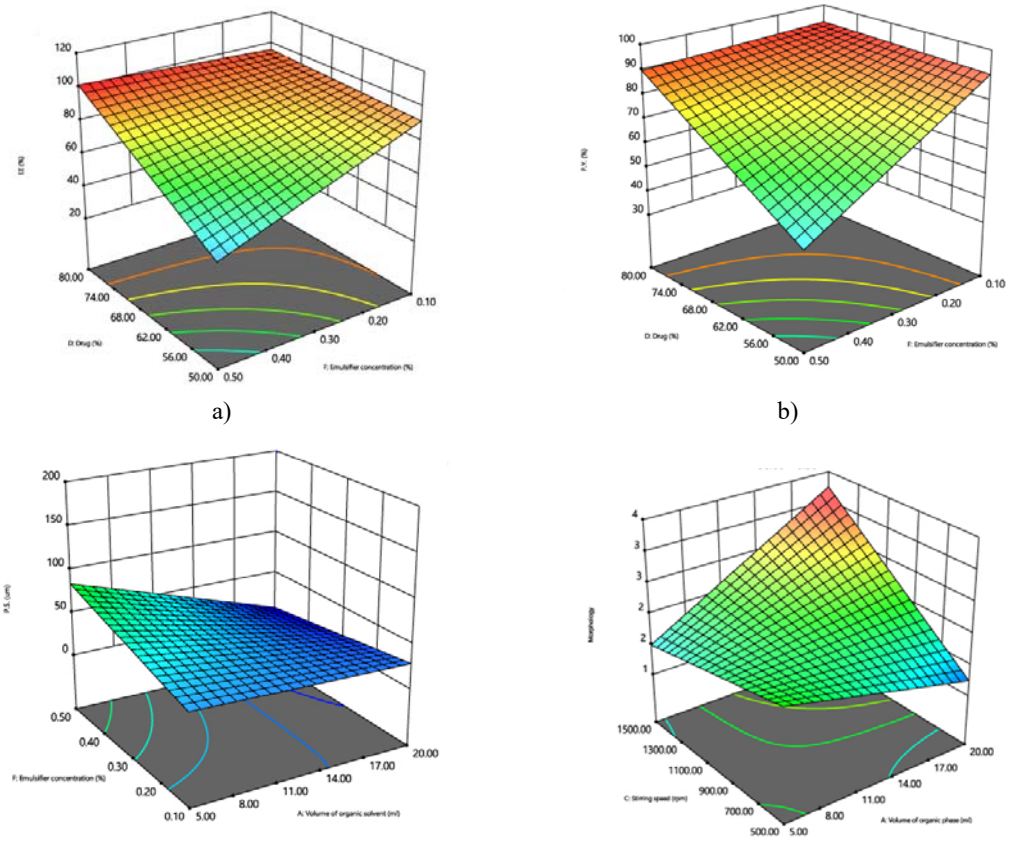

Figure 2. Three-dimensional response surface plots generated from the Plackett-Burman design for the prepared microsponge formulations: (a) entrapment efficiency in relation to drug percentage and emulsifier

concentration (d × f), (b) production yield in terms of D × F, (c) particle size with respect to organic phase volume and stirring speed (a × f), and (d) morphology in terms of a × c. The color gradient from blue to green to red indicates increasing values of the measured response.

High stirring rates have been reported to enhance mechanical shear forces, which promote uniform and rapid dispersion of droplets, thereby facilitating the formation of microsponge particles [24, 41]. In line with this, stirring speed in our study exhibited a direct and significant positive effect on entrapment efficiency. Although sonication time (b) showed no statistically significant influence, a slight positive trend was observed, possibly because prolonged sonication reduces the size of dispersed drug particles, enhancing drug loading within the microsponges [34].

Effect of parameters on production yield (Y2)

Production yield (P.Y.%) reflects the ratio of dry microsponge powder obtained to the total mass of drug and polymer used [26]. Since production yield is closely linked to entrapment efficiency, higher EE% generally corresponds to improved P.Y.%, which explains why the highest yield (93.14%) was observed in F11 and the lowest (33.2%) in F12. The factors influencing yield largely mirrored those affecting EE%.

Drug loading percentage (D) emerged as the most influential variable on P.Y.%. This can be explained by the slower diffusion of dichloromethane from concentrated solutions, mediated by polymer viscosity, which allows extended time for droplet formation and improves overall microsponge yield [24, 42]. Additionally, higher entrapment efficiency directly increases the amount of drug retained in the microspheres, thereby elevating the total yield [34, 35, 43]. Polymer type (E) also significantly affected P.Y.% due to its impact on EE%; formulations containing Ethyl Cellulose, which enhanced EE%, consequently showed higher production yield.

Conversely, emulsifier concentration (F) had a significant negative effect on P.Y.%. While moderate PVA concentrations can slow DCM diffusion and aid droplet formation, excessive PVA may form hydrophobic domains, reducing drug entrapment and thereby lowering overall yield [24, 35, 36]. The interaction between drug percentage and emulsifier concentration (D × F, **Figure 2b**) significantly improved yield, emphasizing the need to balance these factors. Although organic phase volume (A) had a minor negative effect, decreasing the volume slightly improved yield, consistent with previous findings [43].

Effect of parameters on particle size (Y3)

Particle size is a critical attribute of microsponges, as it influences drug release and performance. The prepared ADA-MS formulations exhibited sizes ranging from 14.97 ± 4 µm (f2) to 162.6 ± 37.4 µm (f10). Stirring speed (c) had the strongest effect, showing a significant inverse relationship: increasing stirring rates from 500 to 1500 rpm produced smaller particles due to rapid droplet dispersion and higher kinetic energy, which limited coalescence [24, 26, 34, 41, 44]. Prolonged high-speed agitation can sometimes promote particle aggregation, but in this study, the fixed 2-hour stirring period prevented this effect [35, 45].

Drug loading (d) also positively influenced particle size, likely due to stronger cohesive interactions between hydrophobic ADA molecules and the polymer, which stabilize larger particles [25, 46]. Conversely, increasing the organic phase volume (a) significantly reduced particle size. Higher DCM volumes lower the internal phase viscosity, facilitating the formation of smaller emulsion droplets, whereas more viscous conditions produce larger particles [24, 25, 34, 37, 46, 47].

The interaction between organic phase volume and emulsifier concentration (a × f, **Figure 2c**) was also significant. Even though emulsifier concentration alone was not significant, increasing both DCM volume and PVA concentration synergistically reduced particle size. This effect can be explained by surface tension reduction in the aqueous phase, combined with lower viscosity of the organic phase, promoting smaller emulsion droplets and ultimately smaller microsponge particles [25, 26, 36].

Effect of investigated parameters on morphology (Y4)

SEM analysis **(Figure 1)** revealed that four of the twelve ADA-MS formulations (f2, f6, f7, and f12) exhibited the highest morphology score (3), characterized by a large number of uniform, spherical microsponge particles. Three formulations (f1, f4, and f9) showed intermediate quality (score 2), while the remaining formulations contained predominantly irregular or fragmented particles (score 1). The surfaces of the microsponges were highly

porous, a feature attributed to the evaporation of DCM, and ADA crystals were observed both on the surface and within the core, indicating effective drug encapsulation.

Drug loading percentage (d) emerged as the most significant negative factor affecting morphology; higher drug concentrations reduced the polymer available to encapsulate the drug, leading to less uniform microsponge formation. Additionally, the interaction between organic phase volume and stirring speed (a × c, **Figure 2d**) was significant, although each factor alone was not. Increasing the organic phase volume to 20 mL in combination with a stirring speed of 1500 rpm resulted in improved particle morphology, likely due to the generation of smaller, more uniform emulsion droplets that subsequently solidified into regular microsponge particles [24, 48, 49].

Polymer type (e) had a negligible impact on morphology; however, formulations with the most uniform particles were prepared using Eudragit RS100. This may reflect the polymer's advanced synthetic design, where tailored functional groups contribute to the formation of more elegant microsponge structures [50].

Based on the screening results, the optimal parameters for ADA-MS formulation were identified as a sonication time of 10 minutes, a stirring speed of 1500 rpm, portionwise addition of the organic phase, and 0.1% PVA as the emulsifier. Other variables, including polymer type, organic phase volume, and drug loading, can be further refined in subsequent optimization studies.

In vitro biological activity of selected ADA-MS formulations

To investigate the effect of microsponge encapsulation, two formulations—ADA-MS-EC (F4) and ADA-MS-EUD (F7)—were selected for biological evaluation, as both exhibited comparable characteristics in terms of independent and dependent variables.

Cytotoxicity assay

ADA has previously demonstrated anticancer activity against multiple cancer cell lines, including melanoma lines such as A375 and M14 [21]. In this study, the human epidermoid carcinoma cell line A431 and human melanoma cell line M10 were employed to assess the topical anticancer potential of ADA, ADA-MS-EC, and ADA-MS-EUD by determining their IC50 values (95% CI).

Results from the MTT proliferation assay **(Figure 3, Table 4)** indicated that free ADA exhibited strong cytotoxicity, with IC50 values of 14.54 µg/mL for A431 cells and 38.05 µg/mL for M10 cells. Although ADA appeared more potent against A431 cells, the difference was not statistically significant. This variation may be partly explained by the fact that squamous cell carcinoma can involve chronic immuno-inflammatory processes [51], and ADA is known to possess immunomodulatory activity [18].

Table 4. In vitro cytotoxicity results on different cell lines

Cell Line	Treatment	IC_{50} µg/mL ± S.D.	95% CL
A431	**Adapalene**	14.54 ± 0.86	6.761–31.28
	ADA- MS - EC	16.4 ±1.05	10.54–25.52
	ADA- MS - EUD	2.765 ± 0.22	1.768–4.316*
M10	**Adapalene**	38.05 ± 1.91	15.6–92.77
	ADA- MS - EC	19.72 ± 1.26	15.36–25.32
	ADA- MS - EUD	8.811 ± 0.52	5.257–14.77*

Note: *Significant difference compared with both Adapalene and ADA-MS-EC.

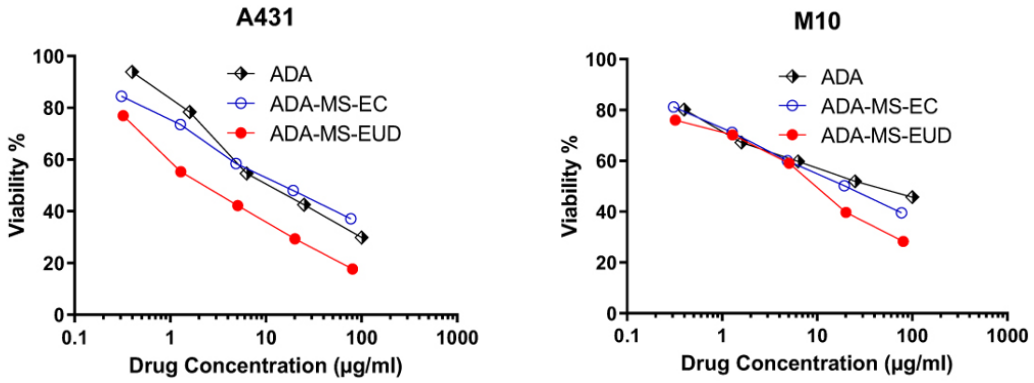

a) b)

Figure 3. Cytotoxicity profiles of free ADA, ADA-MS-EC, and ADA-MS-EUD against A431 and M10 cell lines. The ADA-MS-EC exhibited an IC50 of 16.4 µg/mL on the A431 cell line; although this value was higher than that of free ADA, the difference was not statistically significant. Similarly, the IC50 on the M10 cell line was 19.72 µg/mL, which was lower than that of the pure drug, but the variation was also insignificant. This outcome could be attributed to the encapsulation effect, where the biologically inert Ethyl cellulose polymer forms a matrix that facilitates controlled drug release [52].

Encapsulation of ADA into microsponges (MS) using Eudragit (EUD) significantly reduced the viability of A431 cells compared to both free ADA and ADA-MS-EC, yielding an IC50 of 2.765 µg/mL, which represents a 5.26- and 5.93-fold decrease in IC50, respectively. This notable reduction in cell viability and the enhanced cytotoxic effect of ADA-loaded EUD microsponges prompted further evaluation of EUD alone on the A431 cell line, which demonstrated moderate cytotoxicity with an IC50 of 86 ± 4.38 µg/mL. Likewise, ADA-MS-EUD exhibited a highly significant decrease in the viability of M10 cells, with an IC50 of 8.811 µg/mL, corresponding to a 4.3- and 2.24-fold reduction in IC50. The observed cytotoxic activity of EUD, combined with the increased lipophilicity of microsponges that prolongs cell contact [6], likely contributed to the amplified anticancer effect.

UVA irradiation and cell viability assay

Adapalene has been reported to induce substantial irritation in skin cells upon sunlight exposure [53]. Melanocytes, located in the basal layer of the epidermis, provide the main photoprotective function of the skin [54]. Unlike UVB, UVA radiation penetrates deeper into the skin, reaching the dermal-epidermal junction [55].

Cell viability of HFB-4 cells following UVA exposure was quantified as a percentage relative to the control. From preliminary studies, the cytotoxic dose of ADA on HFB-4 cells was established, and the cells were treated with sub-cytotoxic concentrations of ADA (3, 6, 12 µg/mL), both in free form and within MS formulations (ADA-MS-EUD and ADA-MS-EC). Statistical analysis using two-way ANOVA indicated highly significant differences among all treatments ($p < 0.0001$), among concentrations ($p < 0.0001$), and in the interaction between treatment and concentration ($p = 0.005$), demonstrating that increasing ADA concentration significantly reduced cell viability, consistent with its reported phototoxic effects [56].

One-way ANOVA followed by Tukey's multiple comparisons test for each concentration revealed that ADA-MS-EUD significantly enhanced relative cell viability across all tested doses (90.5 ± 4.59%, 86.5 ± 4.04%, and 80.5 ± 4.91%) compared to free ADA (76 ± 3.18%, 68.9 ± 3.33%, and 64 ± 4.79%) ($p < 0.0005$). Meanwhile, ADA-MS-EC achieved a highly significant increase in relative cell viability (110 ± 3.76%, 112.2 ± 4.62%, and 94.6 ± 5.87%) compared with both ADA and ADA-MS-EUD at all concentrations ($p < 0.0001$), indicating maximal protective effects against UVA-induced cytotoxicity.

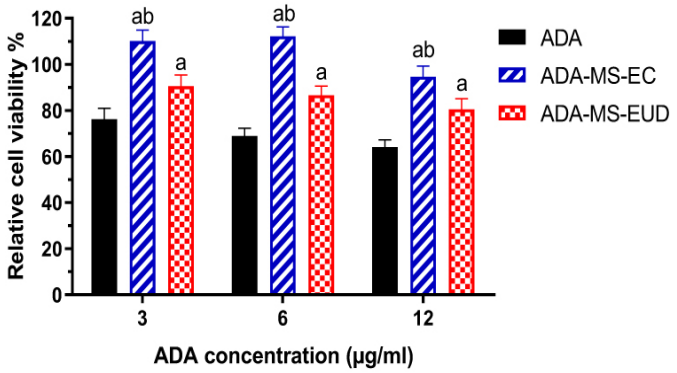

Figure 4. Cell viability assay of HFB-4 cells after UVA irradiation and treatment with different concentrations of free ADA, ADA-MS-EC, and ADA-MS-EUD. For each concentration, results were analyzed using one-way ANOVA followed by Tukey's post hoc test, with ap < 0.0005 compared to the respective ADA relative cell viability and bp < 0.0001 compared to the respective ADA-MS-EUD relative cell viability.

These findings can be attributed to the encapsulation of ADA within the MS formulations, which reduces direct exposure to the full drug dose, thereby significantly minimizing UVA-induced irritation in normal skin cells and enhancing overall cell viability [2, 57]. Moreover, the previously observed slight cytotoxicity of EUD compared to the biologically inert Ethyl cellulose explains the notable differences in relative cell viability between the EUD- and EC-based MS formulations.

Antimicrobial activity assay

To date, ADA's intrinsic antibacterial activity has not been extensively studied [18], although it has been shown to enhance antimicrobial effects when combined with other active ingredients in formulations [32]. In this study, the antimicrobial potential of ADA alone and within MS formulations was evaluated. The minimum inhibitory concentrations (MICs) of ADA, ADA-MS-EC, and ADA-MS-EUD were tested against P. acnes, acknowledging that ADA's primary mechanism in acne treatment is through RAR receptor modulation rather than direct antimicrobial activity.

As depicted in **Figure 5**, linear regression analysis demonstrated that free ADA exhibited antimicrobial activity with an MIC of 235 µg/mL (95% CI: 201.2–275.7). The MS formulations showed reduced MICs: 169.4 µg/mL (95% CI: 126.0–226.2) for ADA-MS-EUD and 163 µg/mL (95% CI: 138.6–190.8) for ADA-MS-EC. While there was no significant difference between ADA and ADA-MS-EUD, a significant difference was observed between ADA and ADA-MS-EC. This improvement in antibacterial activity may result from the hydrophobic polymers of the MS interacting with and destabilizing the microbial membrane, with differences in polymer hydrophobicity accounting for variability in efficacy [58].

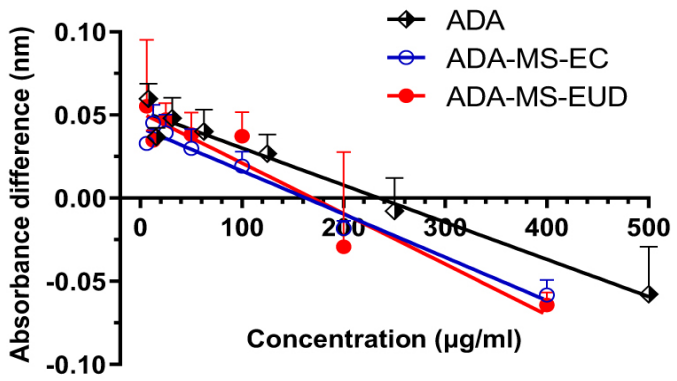

Figure 5. Determination of the minimum inhibitory concentration (MIC) after treatment with varying concentrations of ADA, ADA-MS-EC, and ADA-MS-EUD against P. acnes.

Conclusion

In this study, Adapalene-loaded microsponges were successfully developed using either Ethyl cellulose or Eudragit RS100 as polymeric matrices. The findings demonstrated that multiple formulation and processing parameters markedly influence the characteristics of ADA-MS and can be optimized accordingly. Notably, the microsponges significantly enhanced the cytotoxic activity of ADA against the cancerous A431 and M10 cell lines, while simultaneously providing improved protection to normal HFB-4 cells, along with augmented antibacterial activity against P. acnes. These results suggest that microsponges represent a promising carrier system for ADA delivery, capable of enhancing its in vitro biological performance and supporting further formulation optimization studies.

Acknowledgments: None

Conflict of Interest: None

Financial Support: None

Ethics Statement: None

References

1. Jadhav N, Patel V, Mungekar S, Bhamare G, Karpe M, Kadams V. Microsponge delivery system: an updated review, current status and future prospects. J Sci Innov Res. 2013;2(6):1097–110.
2. Kappor D, Patel M, Vyas RB, Lad C, Tyagi BL. A review on microsponge drug delivery system. J Drug Deliv Therap. 2014;4(5):29–35. doi:10.22270/jddt.v4i5.978
3. Patel EK, Oswal RJ. Nanosponge and micro sponges: a novel drug delivery system. Int J Res Pharm Chem. 2012;2(2):2281–781.
4. Akhgari A, Tavakol A. Prediction of optimum combination of Eudragit RS/Eudragit RL/ethyl cellulose polymeric free films based on experimental design for using as a coating system for sustained release theophylline pellets. Adv Pharm Bull. 2016;6(2):219. doi:10.15171/apb.2016.030
5. Singhvi G, Manchanda P, Hans N, Dubey SK, Gupta G. Microsponge: an emerging drug delivery strategy. Drug Dev Res. 2019;80(2):200–8. doi:10.1002/ddr.21492
6. Mahant S, Kumar S, Nanda S, Rao R. Microsponges for dermatological applications: perspectives and challenges. Asian J Pharm Sci. 2020;15(3):273–91. doi:10.1016/j.ajps.2019.05.004
7. Lewis GA, Mathieu D, Phan-Tan-Luu R. Mixtures in a constrained region of interest. In: pharmaceutical experimental design. New York: Marcel Dekker; 1999:413–54.
8. Rahman Z, Zidan AS, Habib MJ, Khan MA. Understanding the quality of protein loaded PLGA nanoparticles variability by Plackett–Burman design. Int J Pharm. 2010;389(1–2):186–94. doi:10.1016/j.ijpharm.2009.12.040
9. Singh B, Ahuja N. Pharmaceutical experimental design (Drugs and the Pharmaceutical Sciences, Vol. 92), Edited by GA Lewis, D. Mathieu and R. Phan-Tan-Luu, Marcel Dekker, New York, 1999. vi+ 498 pp., 23.5 x15. 5 cm., 1.9 lb., Hardcover, ISBN 0-8247-9860-0, Price $175.00. Int J Pharm. 2000;195(1–2):247–8. doi:10.1016/S0378-5173(99)00384-1
10. Plackett RL, Burman JP. The design of optimum multifactorial experiments. Biometrika. 1946;33(4):305–25. doi:10.1093/biomet/33.4.305
11. El-Say KM, Abdelaziz AE, Samy AM, Kassem AA. Screening study for formulation variables in preparation of diclofenac sodium niosomes using Plackett – Burman design. Azhar J Pharma Sci. 2008;38:36–53.
12. Badawi N, El-Say K, Attia D, El-Nabarawi M, Elmazar M, Teaima M. Development of pomegranate extract-loaded solid lipid nanoparticles: quality by design approach to screen the variables affecting the quality attributes and characterization. ACS Omega. 2020;5(34):21712–21. doi:10.1021/acsomega.0c02618
13. Jayakumar M. When and how to use Plackett-Burman experimental design. iSixSigma; 2013. Available from: https://www.isixsigma.com/tools-templates/design-of-experiments-doe/when-and-how-to-use-plackett-burman-experimental-design/. Accessed September 10, 2022.

14. Irby CE, Yentzer BA, Feldman SR. A review of adapalene in the treatment of acne vulgaris. J Adolesc Health. 2008;43(5):421–4. doi:10.1016/j.jadohealth.2008.06.005
15. Waugh J, Noble S, Scott LJ. Adapalene. Drugs. 2004;64(13):1465–78. doi:10.2165/00003495-200464130-00005
16. Czernielewski J, Michel S, Bouclier M, Baker M, Hensby C. Adapalene biochemistry and the evolution of a new topical retinoid for treatment of acne. J Eur Acad Dermatol Venereol. 2001;15(3):5–12. doi:10.1046/j.0926-9959.2001.00006.x
17. Piskin S, Uzunali E. A review of the use of Adapalene for the treatment of acne vulgaris. Ther Clin Risk Manag. 2007;3(4):621.
18. Rusu A, Tanase C, Pascu GA, Todoran N. Recent advances regarding the therapeutic potential of Adapalene. Pharmaceuticals. 2020;13(9):217. doi:10.3390/ph13090217
19. Treesirichod A, Chaithirayanon S, Wongjitrat N, Wattanapan P. The efficacy of topical 0.1% Adapalene gel for use in the treatment of childhood acanthosis nigricans: a pilot study. Indian J Dermatol. 2015;60(1):103. doi:10.4103/0019-5154.147838
20. Herane MI, Orlandi C, Zegpi E, Valdés P, Ancić X. Clinical efficacy of Adapalene (Differin®) 0.3% gel in Chilean women with cutaneous photoaging. J Dermatol Treat. 2012;23(1):57–64. doi:10.3109/09546634.2011.631981
21. Li H, Wang C, Li L, Bu W, Zhang M, Wei J, et al. Adapalene suppressed the proliferation of melanoma cells by S-phase arrest and subsequent apoptosis via induction of DNA damage. Eur J Pharmacol. 2019;851:174-85. doi:10.1016/j.ejphar.2019.03.004. Epub 2019 Mar 2. PMID: 30836068.
22. Lauterbach A, Mueller-Goymann CC. Development, formulation, and characterization of an Adapalene-loaded solid lipid microparticle dispersion for follicular penetration. Int J Pharm. 2014;466(1–2):122–32. doi:10.1016/j.ijpharm.2014.02.050
23. Jelvehgari M, Siahi-Shadbad MR, Azarmi S, Martin GP, Nokhodchi A. The microsponge delivery system of benzoyl peroxide: preparation, characterization and release studies. Int J Pharm. 2006;308(1–2):124–32. doi:10.1016/j.ijpharm.2005.11.001
24. Salah S, Awad GEA, Makhlouf AIA. Improved vaginal retention and enhanced antifungal activity of miconazole microsponges gel: formulation development and in vivo therapeutic efficacy in rats. Eur J Pharma Sci. 2018;114:255–66. doi:10.1016/j.ejps.2017.12.023
25. Patel N, Padia N, Vadgama N, Raval M, Sheth N. Formulation and evaluation of microsponge gel for topical delivery of fluconazole for fungal therapy. J Pharm Investig. 2016;46(3):221–38. doi:10.1007/s40005-016-0230-7
26. Ivanova NA, Trapani A, Franco CD, Mandracchia D, Trapani G, Franchini C, et al. In vitro and ex vivo studies on diltiazem hydrochloride-loaded microsponges in rectal gels for chronic anal fissures treatment. Int J Pharm. 2019;557:53-65. doi:10.1016/j.ijpharm.2018.12.039. Epub 2018 Dec 21. PMID: 30580086.
27. Badawi NM, Teaima MH, El-Say KM, Attia DA, El-Nabarawi MA, Elmazar MM. Pomegranate extract-loaded solid lipid nanoparticles: design, optimization, and in vitro cytotoxicity study. Int J Nanomedicine. 2018;13:1313. doi:10.2147/IJN.S154033
28. Park JG, Son YJ, Aravinthan A, Kim JH, Cho JY. Korean Red Ginseng water extract arrests growth of xenografted lymphoma cells. J Ginseng Res. 2016;40(4):431–6. doi:10.1016/j.jgr.2016.07.006
29. Chen SJ, Hseu YC, Gowrisankar YV, Chung YT, Zhang YZ, Way TD, et al. The anti-melanogenic effects of 3-O-ethyl ascorbic acid via Nrf2-mediated α-MSH inhibition in UVA-irradiated keratinocytes and autophagy induction in melanocytes. Free Radic Biol Med. 2021;173:151-69. doi:10.1016/j.freeradbiomed.2021.07.030. Epub 2021 Jul 24. PMID: 34314818.
30. Ryu BM, Qian ZJ, Kim MM, Nam KW, Kim SK. Anti-photoaging activity and inhibition of matrix metalloproteinase (MMP) by marine red alga, Corallina pilulifera methanol extract. Radiat Phys Chem. 2009;78(2):98–105. doi:10.1016/j.radphyschem.2008.09.001
31. Najafi-Taher R, Ghaemi B, Amani A. Delivery of adapalene using a novel topical gel based on tea tree oil nano-emulsion: permeation, antibacterial and safety assessments. Eur J Pharma Sci. 2018;120:142–51. doi:10.1016/j.ejps.2018.04.029
32. Shamma RN, Ad-din IS, Abdeltawab NF. Dapsone-gel as a novel platform for acne treatment: in vitro evaluation and In vivo performance and histopathological studies in acne infected mice. J Drug Deliv Sci Technol. 2019;54:101238. doi:10.1016/j.jddst.2019.101238

33. Thiruchelvi R, Venkataraghavan R, Sharmila D. Optimization of environmental parameters by Plackett-Burman design and response surface methodology for the adsorption of malachite green onto gracilaria edulis. Mater Today Proc. 2020;37(Part 2):1859–64. doi:10.1016/j.matpr.2020.07.448
34. Obiedallah MM, Abdel-Mageed AM, Elfaham TH. Ocular administration of acetazolamide microsponges in situ gel formulations. Saudi Pharm J. 2018;26(7):909–20. doi:10.1016/j.jsps.2018.01.005
35. Moin A, Deb T, Osmani RM, Bhosale R, Hani U. Fabrication, characterization, and evaluation of microsponge delivery system for facilitated fungal therapy. J Basic Clin Pharm. 2016;7(2):39. doi:10.4103/0976-0105.177705
36. Devi N, Kumar S, Prasad M, Rao R. Eudragit RS100 based microsponges for dermal delivery of clobetasol propionate in psoriasis management. J Drug Deliv Sci Technol. 2020;55:101347. doi:10.1016/j.jddst.2019.101347
37. Pandit AP, Patel SA, Bhanushali VP, Kulkarni VS, Kakad VD. Nebivolol-loaded microsponge gel for healing of diabetic wound. AAPS PharmSciTech. 2017;18(3):846–54. doi:10.1208/s12249-016-0574-3
38. Shahzad Y, Saeed S, Ghori MU, Mahmood T, Yousaf AM, Jamshaid M, et al. Influence of polymer ratio and surfactants on controlled drug release from cellulosic microsponges. Int J Biol Macromol. 2018;109:963-970. doi:10.1016/j.ijbiomac.2017.11.089. Epub 2017 Nov 14. PMID: 29154881.
39. Orlu M, Cevher E, Araman A. Design and evaluation of colon specific drug delivery system containing flurbiprofen microsponges. Int J Pharm. 2006;318(1–2):103–17. doi:10.1016/j.ijpharm.2006.03.025
40. Deshmukh K, Poddar SS. Tyrosinase inhibitor-loaded microsponge drug delivery system: new approach for hyperpigmentation disorders. J Microencapsul. 2012;29(6):559–68. doi:10.3109/02652048.2012.668955
41. Jain V, Singh R. Dicyclomine-loaded eudragit®-based microsponge with potential for colonic delivery: preparation and characterization. Trop J Pharma Res. 2010;9(1):67–72. doi:10.4314/tjpr.v9i1.52039
42. Lee JH, Park TG, Choi HK. Development of oral drug delivery system using floating microspheres. J Microencapsul. 1999;16(6):715–29. doi:10.1080/026520499288663
43. Junqueira MV, Calçado SC, de Castro-Hoshino LV, Baesso ML, Szarpak-Jankowska A, Auzély-Velty R, et al. Influence of the ethanol/dichloromethane ratio on the preparation of microsponges composed of ethylcellulose and Eudragit or HPMCphthalate for hydrophilic drug delivery. J Mol Liq. 2020;303:112633.
44. Kumari A, Jain A, Hurkat P, Tiwari A, Jain SK. Eudragit S100 coated microsponges for Colon targeting of prednisolone. Drug Dev Ind Pharm. 2018;44(6):902–13. doi:10.1080/03639045.2017.1420079
45. Behan N, O'Sullivan C, Birkinshaw C. Synthesis and in-vitro drug release of insulin-loaded poly (n-butyl cyanoacrylate) nanoparticles. Macromol Biosci. 2002;2(7):336–40. doi:10.1002/1616-5195(200209)2:7<336::AID-MABI336>3.0.CO;2-P
46. Nagula RL, Wairkar S. Cellulose microsponges based gel of naringenin for atopic dermatitis: design, optimization, in vitro and in vivo investigation. Int J Biol Macromol. 2020;164:717–25. doi:10.1016/j.ijbiomac.2020.07.168
47. Othman MH, Zayed GM, El Sokkary GH, Ali UF, Abdellatif AA. Preparation and evaluation of 5-fluorouracil loaded microsponges for treatment of colon cancer. J Cancer Sci Ther. 2017;9(1). doi:10.4172/1948-5956.1000433
48. Mishra MK, Shikhri M, Sharma R, Goojar MP. Optimization, formulation development and characterization of Eudragit RS 100 loaded microsponges and subsequent colonic delivery. Int J Drug Discov Herbal Res. 2011;1(1):8–13.
49. Perumal D. Microencapsulation of ibuprofen and Eudragit® RS 100 by the emulsion solvent diffusion technique. Int J Pharm. 2001;218(1–2):1–11. doi:10.1016/S0378-5173(00)00686-4
50. Cilurzo F, Selmin F, Gennari CG, Montanari L, Minghetti P. Application of methyl methacrylate copolymers to the development of transdermal or loco-regional drug delivery systems. Expert Opin Drug Deliv. 2014;11(7):1033–45. doi:10.1517/17425247.2014.912630
51. Feller L, Khammissa RAG, Kramer B, Altini M, Lemmer J. Basal cell carcinoma, squamous cell carcinoma and melanoma of the head and face. Head Face Med. 2016;12(1). doi:10.1186/s13005-016-0106-0
52. Arya P, Pathak K. Assessing the viability of microsponges as gastro retentive drug delivery system of curcumin: optimization and pharmacokinetics. Int J Pharm. 2014;460(1–2):1–12. doi:10.1016/j.ijpharm.2013.10.045

53. Vasanth S, Dubey A, G S R, Lewis SA, Ghate VM, El-Zahaby SA, et al. Development and investigation of vitamin C-enriched adapalene-loaded transfersome gel: a collegial approach for the treatment of acne vulgaris. AAPS PharmSciTech. 2020;21(2):61. doi:10.1208/s12249-019-1518-5. PMID: 31915948.
54. Cichorek M, Wachulska M, Stasiewicz A, Tymińska A. Skin melanocytes: biology and development. Postepy Dermatol Alergol. 2013;1(1):30–41. doi:10.5114/pdia.2013.33376
55. Arisi M, Zane C, Caravello S, Rovati C, Zanca A, Venturini M, et al. Sun exposure and melanoma, Certainties and weaknesses of the present knowledge. Front Med (Lausanne). 2018;5:235. doi:10.3389/fmed.2018.00235. PMID: 30214901; PMCID: PMC6126418.
56. Thielitz A, Gollnick H. Topical retinoids in acne vulgaris update on efficacy and safety. Am J Clin Dermatol. 2008;9:369–81. doi:10.2165/0128071-200809060-00003
57. Ramezanli T, Zhang Z, Michniak-Kohn BB. Development and characterization of polymeric nanoparticle-based formulation of adapalene for topical acne therapy. Nanomedicine. 2017;13(1):143–52. doi:10.1016/j.nano.2016.08.008
58. Tan J, Zhao Y, Hedrick JL, Yang YY. Effects of hydrophobicity on antimicrobial activity, selectivity, and functional mechanism of guanidinium-functionalized polymers. Adv Healthc Mater. 2021. doi:10.1002/adhm.202100482